

Synchronization of surface reactions via Turing-like structures

R. Salazar and A. P. J. Jansen

Schuit Institute of Catalysis (ST/SKA), Eindhoven University of Technology, P.O. Box 513, 5600 MB Eindhoven, The Netherlands

V. N. Kuzovkov

Institute for Solid State Physics, University of Latvia, Kengaraga 8, LV-1063, Riga, Latvia

(Received 13 November 2003; published 30 March 2004)

We discuss an alternative to the traditional gas-phase coupling approach in order to explain synchronized global oscillations in CO oxidation on Pt(110). We use a microscopic model which includes structural Pt surface reconstruction via front propagation, and large diffusion rates for CO. The synchronization mechanism is associated with the formation of a Turing-like structure of the substrate. By using large parallel microscopic simulations we derive scaling laws which allow us to extrapolate to realistic diffusion rates, pattern size, and oscillation periods.

DOI: 10.1103/PhysRevE.69.031604

PACS number(s): 82.65.+r; 02.70.Tt; 82.20.Wt; 82.40.Np

The nonlinear kinetics of reactions on surfaces can show a variety of phenomena such as many kinds of pattern formation, global oscillations, and even chaotic behavior. Explaining the nonlinear kinetics of surface processes first involves finding out the sequence of processes or reactions that yields time-dependent reaction rates (e.g. an oscillation). For many systems such a sequence is known. For example, in the generally accepted mechanism for CO oxidation on Pt(100) and Pt(110) the crucial characteristic is the reconstruction of the surface [1,2]. This reconstruction can be lifted by the adsorption of CO. The existence of an oscillatory cycle in itself does not determine the kinetics. For most reaction conditions, and possibly even always, it occurs everywhere on the surface but out of phase. The result is either a normal equilibrium or steady state, or some form of pattern formation. To obtain a global oscillation the phases of the local oscillations need to be synchronized.

Two theoretical approaches have been used to study the synchronization mechanism: one uses reaction-diffusion equations, the other simulations. Reaction-diffusion equations are generally employed to model experiments. The procedure consists of finding mathematical expressions describing the processes on the surface to reproduce the experimental data. We find such a top-down phenomenological approach somewhat unsatisfactory, because it is not clear how the mathematical expressions for some reactions arise from the microscopic process they are supposed to describe [3–6].

Simulations form a bottom-up approach in which, first, a microscopic model of a system is made. That model is simulated and the results are compared with experimental data. Such an approach has the advantage that it is very clear what the relation is between the microscopic processes and the macroscopic kinetics. The disadvantage is that this approach is computationally very intensive, and it is therefore hard to obtain an overview of all the properties of a model.

Although the mechanism with the surface reconstruction described above is now generally accepted, this is not the case with the synchronization mechanism [7–9]. Diffusion of CO over the surface is known to be fast, but not fast enough, as it has been noted that the length that CO diffuses during one oscillation period is much smaller than the size of

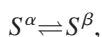
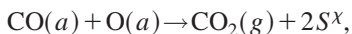
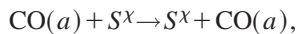
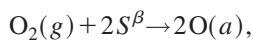
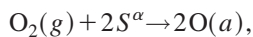
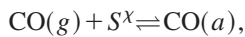
the system in experiments. Therefore, the faster diffusion through the gas phase has been proposed as an alternative mechanism [2,5]. However, theoretical work using only gas phase synchronization based on reaction-diffusion equations indicates that noise can easily nullify gas-phase synchronization [10]. This suggests that it might not be the only operative mechanism. It may not be even the most important one. Reaction-diffusion equation modeling of this synchronization mechanism has also predicted other properties not in agreement with experiment [8,9].

Recent work on simulations of a model of CO oxidation have shown that synchronization can also be obtained with only surface processes [7,11]. The model uses spontaneous reconstruction and a lifting of that reconstruction. If diffusion of CO is so fast that CO can move from one site, where such a spontaneous process occurs, to another within one oscillatory period, then stochastic resonance is obtained and the oscillations become global. In fact this can be observed even with quite slow CO diffusion and global oscillations were easily obtained with this model. In particular for Pt(110), oscillations are only found in a very narrow parameter interval [2]. It is therefore unlikely, at least for Pt(110), that this mechanism is operative.

In this paper we present results of Monte Carlo (MC) simulations for CO oxidation on Pt(110) using the same model as the one showing stochastic resonance [7,11], but we have removed the spontaneous reconstructions. We will show that the model still can give global oscillations, but only for restricted reaction conditions, as is also found experimentally. The surface reconstructs and forms Turing-like structures with a definite width. The diffusion length needs only to exceed that width to obtain global oscillations. If the diffusion is slower, we get pattern formation in the adlayer. These patterns also have a characteristic length scale, which is, however, different from that of the Turing-like structures which are present at the same time. So we present a synchronization mechanism without gas-phase coupling, coupling via stochastic resonance, or lateral interactions, which yields global oscillations or pattern formation as observed experimentally. In addition we provide a connection between these MC simulations and experimental results, via scaling laws.

MC simulations provide a systematic approach to include microscopic effects [12]. The MC method directly simulates the chemical reaction steps in a model, without averaging out particle correlations. Simulations of our model were performed by using a cellular automaton, which has been shown to be equivalent to MC simulations [7,13]. A limitation of MC simulations has been the inability to deal with experimental system sizes and realistic diffusion coefficients. However, by using large parallel simulations we can now estimate results for experimental conditions. Using this parallel code we are able to simulate system sizes of about $1 \mu\text{m}$ with diffusion coefficients of about $10^{-10} \text{ cm}^2 \text{ sec}^{-1}$. This approaches experimental conditions more closely than any previous MC simulation, to our knowledge. Experimental values are for system sizes of $10^2 \mu\text{m}$ or more, and the diffusion coefficient $10^{-6} \text{ cm}^2 \text{ sec}^{-1}$. There is a gap between experimental and simulated rate constants, but, as we can vary the system size and the diffusion rate over a large range, we can derive scaling laws which we can use to extrapolate the behavior predicted by our model to realistic system sizes and diffusion rates.

Our model has already been used in several studies [7,13,14]. CO is able to adsorb onto a free surface site with a rate constant y , and it desorbs from the surface with a rate constant k . Both reactions are independent of the surface phase to which the site belongs. In addition CO is able to diffuse via hopping onto a vacant nearest neighbor site with rate constant D . O_2 adsorbs dissociatively onto two nearest neighbor sites with a rate constant $(1-y)s_\chi$ with $\chi=\alpha,\beta$, where α denotes the 1×2 phase and β denotes the unreconstructed 1×1 phase of Pt(110) [2]. The experimental value for the ratio of the sticking coefficients of O_2 on the two phases is $s_\alpha:s_\beta\approx 0.5:1$. The smaller sticking coefficient for the α phase leads to a displacement of oxygen by CO on α . The $\text{CO}+\text{O}\rightarrow\text{CO}_2$ reaction occurs with a rate constant R , when CO and O are on nearest-neighbor sites. CO_2 desorbs immediately, forming two vacant sites. The $\alpha\rightleftharpoons\beta$ surface phase transition is modeled as a front propagation with a rate constant V . For two nearest-neighbor surface sites in the state $\alpha\beta$ the transition $\alpha\beta\rightarrow\alpha\alpha$ ($\alpha\beta\rightarrow\beta\beta$) occurs if none (at least one) of these two sites is occupied by CO. So without CO the substrate reconstructs to the α phase, and with CO this reconstruction is lifted and the substrate converts to the β phase. Together with the difference of s_α and s_β this causes the oscillations. Summarizing the above transitions and writing them in the more usual form of reaction equations gives



where S stands for a vacant adsorption site, χ stands for either α or β , and (a) and (g) stand for a particle adsorbed on the surface or in the gas phase, respectively. For additional details see Ref. [13]. The rate constants mentioned above have been normalized. The adsorption rate for CO is related to the partial pressures by $y = P_{\text{CO}}/(P_{\text{CO}} + P_{\text{O}_2})$. Comparing our rate constants with typical experimental values used in models using reaction-diffusion equation we can estimate the unit of time in our simulations to be about $t_0 \approx 10^{-2} \text{ sec}$ [6,15]. All our rate constants are expressed in that unit of time. Lengths are expressed in units of the unit cell parameter a . The diffusion rate D is related to the experimental diffusion coefficient D_A by $D_A = a^2 D / z t_0$, where $z=4$ is the coordination number.

The quality of the oscillations as a function of y has a typical resonance form. Well-defined oscillations are found near $y=0.494$. Under certain conditions, which we discuss below, these oscillations are global. Moving away from $y=0.494$ we see first that the synchronization decreases and then a disappearance of the oscillations. We restrict ourselves to $y=0.494$ (for a fixed values $k=0.1$ and $V=1$) in our simulations.

We have found that two situations are possible depending on the system size, the diffusion rate, and the initial conditions. If the system is small or the diffusion is fast we find global oscillations. If the diffusion is too slow for a given system size the initial conditions become important. We can again have global oscillations or the formation of patterns in the form of moving fronts and spirals. To illustrate the synchronization mechanism, Fig. 1 shows global oscillations. When the system is covered almost fully by CO the β islands in the α background grow (snapshots 1 and 2). When the size of the β islands is large enough the rate of adsorption of O_2 becomes larger than the adsorption of CO on the β zones (snapshots 3 and 4). At the same time the CO in the α zones is converted to CO_2 near to the borders with the β zones (snapshot 4). When the total coverage of oxygen becomes larger than CO, the direction of the island growth is reversed (snapshots 4, 5, and 6) and α islands grow in the β background. When the size of the β zones is not large enough to keep the oxygen coverage larger than the CO coverage (snapshot 7), then both phases become covered by CO, and the cycle starts again (snapshot 8). The key point in this cycle is the existence of a critical size of the β islands where oxygen becomes more stable than CO and a critical size of α islands where CO is more stable than oxygen. This corresponds to a phase transition produced by varying the size of these islands. This phase transition is driven by diffusion and the critical size of the islands depends on the diffusion rate as \sqrt{D} .

We found that the most important feature of the structures of the substrate is the typical distance between the islands; i.e., the correlation length l_c of these structures. For l_c we use the distance to the first maximum in the radially averaged correlation function of the substrate. The shape of the islands self-organizes through successive oscillations until the whole system is covered with same-sized islands separated by similar distances. We note that the few simple reac-

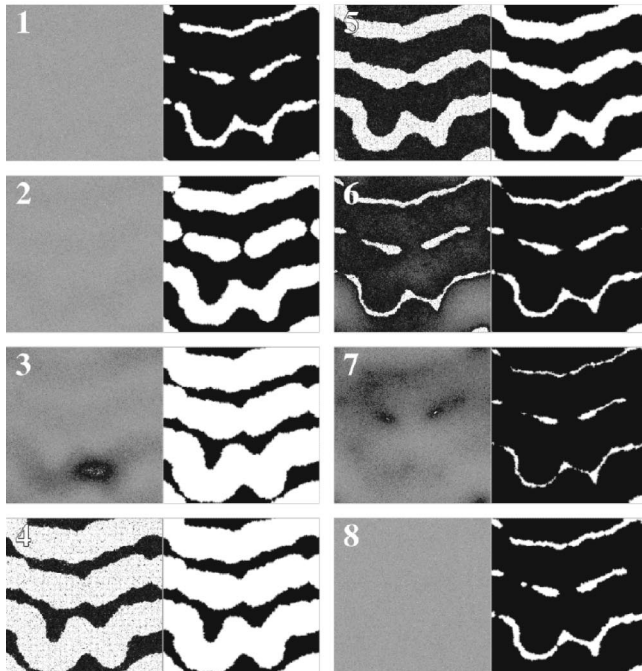
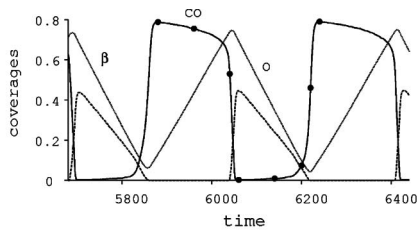


FIG. 1. Oscillations for $D=4000$ and $L=1024$ on the coverage CO, oxygen, and β . Sequence of temporal snapshots correspond to the points in the upper figure. Each snapshot has two parts: In the left part we plot the chemical species; CO particles are gray and O particles are white, and empty sites are black. The right part shows the structure of the surface; α phase sites are black, and β phase sites are white.

tions in our model are sufficient to produce this effect. It yields synchronization at large scales even with relatively small diffusion rates. In Fig. 1 the diffusion length $\xi = \sqrt{DT}$, with T the period of the oscillations, is larger than the system size L . The synchronization is therefore trivial. In Fig. 2, however, a simulation is shown on the left where the diffusion length is much smaller than the lattice size, but larger than the correlation length. So the diffusion synchronizes the oscillations on neighboring islands, and the self-organization leads to global oscillations. If we have synchronized oscillations and then reduce the diffusion so that the diffusion length becomes less than the correlation length, then the oscillations may persist for many periods but eventually we get pattern formation (see below).

In cases where the synchronization is even better, as with large D values, islands tend to group and form rolls which are parallel (see Fig. 1). The structures formed in this way resemble labyrinthine Turing structures. Moreover a percolating connection between islands can be observed. The full analytical analysis of this behavior is far from trivial. However, the difference of the mobility for CO and O could be

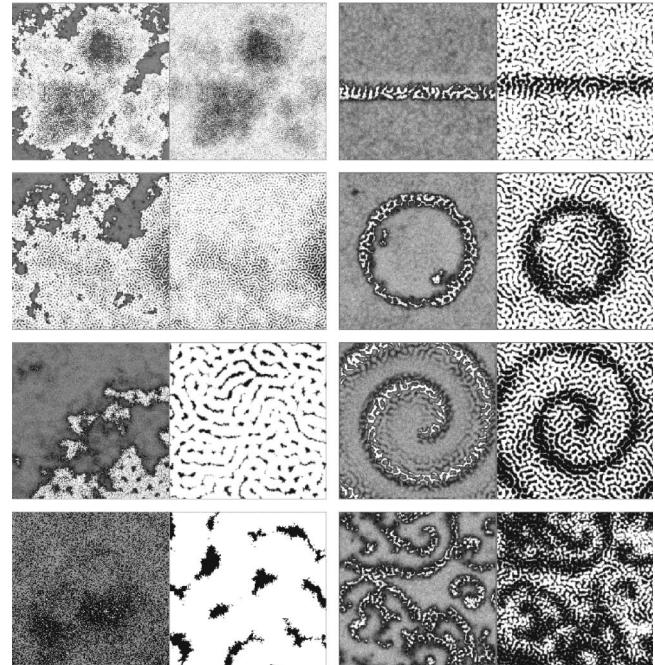
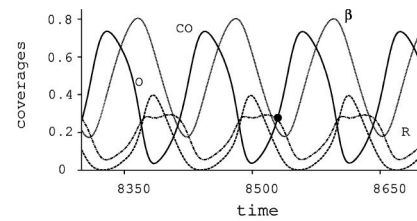


FIG. 2. Global oscillations and pattern formation with $D=250$. The whole system ($L=8192$) and sections of the upper-left corner with $L=4096, 1024$, and 256 are shown on the left side. The snapshots correspond to the dot in the temporal plot at the top. It shows the same information as Fig. 1, but it also includes the rate of CO_2 formation R . On the right side we have a wave front, a target, a spiral, and turbulence (all from simulations with $L=2048$), which can be obtained with different initial conditions.

sufficient for getting a Turing instability in this model.

Pattern formation can also occur when the diffusion is slow, as on the right side of Fig. 2. If we start with a bare surface we usually obtain the turbulent pattern, as shown in the bottom-right part of Fig. 2. If we start, however, with CO forming a wave front, circle, or spiral, then this leads to the stable patterns in the other snapshots on the right of Fig. 2. In each case the substrate is initially a random mixture of α and β sites. The distance between the centers of α and β islands during pattern formation is the same as for the global oscillations, but the sizes of the islands differ for different parts of the system. These differences will not be removed as in the fully synchronized cases. As a consequence a delay or detuning will appear in the oscillations for different parts of the surface, which can create fronts, target patterns, spirals, and turbulence. A cross section of one of these fronts shows a delay between the pulse of the adsorbates and the pulse of the substrate phases. The delay determines the direction of propagation. This is a common feature of excitable bistable systems such as the activator-inhibitor models. The most re-

markable feature is that these fronts appear on top of fixed Turing-like structures which are present even in these incompletely synchronized cases. So within our model we have two different length scales for pattern formation: excitable dynamics for fronts and spirals on a mesoscopic scale (Hopf instability [6]), and a quasifixed Turing-like microscopic structure.

We have made a scaling analysis for the period of oscillations T and the correlation length l_c as a function of diffusion rate D . Numerically we found that the relations $T(D) \sim D^\nu$ and $l_c(D) \sim D^\mu$ hold with $\nu=0.4849 \pm 0.016$ and $\mu=0.5069 \pm 0.01$. For large D a large system size is required to compute $l_c(D)$ precisely. For instance for $D=8000$ we use $L=8192$. Additionally large diffusion rates means that most of the time is spent moving particles; on 8000 diffusion steps only one chemical reaction happens. Also the simulation time increases because the oscillation period increases with D .

A relationship $T(D) \sim l_c(D) \sim D^{1/2}$ seems quite reasonable, as our model has fast diffusion. In fact the scaling law for l_c is a consequence of the scaling law for T . The width of the Turing structure oscillates on a length of order l_c due to the phase propagation with rate V . The period is related to these by $l_c \sim VT$. If the velocity V is constant, then $l_c \sim T$. Using a larger value for the velocity parameter we can obtain larger correlation lengths l_c and smaller periods T , but the scaling remains the same. We have found for the Turing-synchronized oscillations that the relation $T \sim V^{-1/2}$ also applies as in Refs. [7,11,13]. So we have an important scaling law in form $T = c\sqrt{D/V}$ with $c \sim 10$. Realistic diffusion rates of $D_A \sim 10^{-6} \text{ cm}^2 \text{ sec}^{-1}$ give $D \sim 10^8$. The experimental oscillations period is $\tau = t_0 T$ with $t_0 \sim 10^{-2} \text{ sec}$ and $\tau = 100 \text{ sec}$. The value V predicted by our model for that value of τ is then of the order of $V \sim 10^2$.

We propose that the minimal condition to have global oscillations is that the diffusion length ξ is at least of the order of the correlation length l_c : $\xi = l_c$. As we are only interested in orders of magnitude we set $\xi = \sqrt{DT}$ and $l_c = VT$. Critical values for the diffusion rate and the correlation length are then

$$\begin{aligned} D &= c^2 V^3, \\ l_c &= c^2 V^2, \end{aligned} \quad (1)$$

with $c \sim 10$. For $V=1$ we get the order of the parameters used in Fig. 2 (left side), $D \sim 10^2$ and $l_c \sim 10^2$, where global oscillations are possible but infrequent.

Diffusion is a thermally activated process so we can compare our proposal [Eqs. (1)] with the experimental crossover at $T \sim 500$. For lower temperatures where fronts and spirals appear we have low diffusion rates, $\xi < l_c$, and the synchronization mechanism is not stable and produces patterns similar to those on the right of Fig. 2. On the other hand, for large temperatures where standing waves and chemical turbulence appear, we have large diffusion rates, $\xi > l_c$, and we get better synchronization, as in Fig. 1. For $\xi = l_c$ we get the crossover, Eqs. (1) holds, and we get the minimum criteria for synchronization, as in Fig. 2 on the left.

Using $V=10^2$ in Eqs. (1) for the critical value of the diffusion rate we get $D \sim 10^8$, which corresponds to the experimental value of $D_A \sim 10^{-6} \text{ cm}^2 \text{ sec}^{-1}$. This confirms our crossover idea. For correlation length $l_c \sim 10^6$ (in units of cell parameter a) we have a size $\sim 10^2 \mu\text{m}$ which is of the order of magnitude of the standing waves observed in experiments [15]. Near crossover it is possible also to interpret V as the velocity v of the fronts and spirals. For $V=10^2$ we have $v = aV/t_0 \sim 10^{-4} \text{ cm s}^{-1}$, in agreement with experiments [4].

To summarize, in this paper we have presented a mechanism for the synchronization of global oscillations based on microscopic Turing-like structures in the reconstruction of the surface. In cases with incomplete synchronized oscillations the adlayer has a mesoscopic second characteristic length. To our knowledge this is the first actual demonstration of a double length scale. Scaling laws are analyzed to connect the model to experimental parameter values.

This work was supported by the Nederlandse Organisatie voor Wetenschappelijk Onderzoek (NWO). We would like to thank the National Research School Combination Catalysis (NRSCC) for computational facilities. V.N.K. gratefully acknowledges the support of the Deutsche Forschungsgemeinschaft.

-
- [1] M. M. Slin'ko and N. I. Jaeger, *Oscillating Heterogeneous Catalytic Systems, Studies in Surface Science and Catalysis 86* (Elsevier, Amsterdam, 1994).
- [2] R. Imbihl and G. Ertl, *Chem. Rev. (Washington, D.C.)* **95**, 697 (1995).
- [3] K. Krischer, M. Eiswirth, and G. Ertl, *J. Chem. Phys.* **96**, 9161 (1992).
- [4] M. Falcke, M. Bär, H. Engel, and M. Eiswirth, *J. Chem. Phys.* **97**, 4555 (1992).
- [5] M. Falcke and H. Engel, *Phys. Rev. E* **50**, 1353 (1994).
- [6] M. Bär, M. Hildebrand, M. Eiswirth, M. Falcke, H. Engel, and M. Neufeld, *Chaos* **4**, 499 (1994).
- [7] O. Kortlüke, V.N. Kuzovkov, and W. von Niessen, *Phys. Rev. Lett.* **83**, 3089 (1999).
- [8] J. Verdasca, P. Borckmans, and G. Dewel, *Phys. Rev. E* **64**, 055202 (2001).
- [9] J. Verdasca, P. Borckmans, and G. Dewel, *Phys. Chem. Chem. Phys.* **8**, 1355 (2002).
- [10] M. Hildebrand, *Chaos* **12**, 144 (2002).
- [11] O. Kortlüke, V.N. Kuzovkov, and W. von Niessen, *Phys. Rev. E* **66**, 036139 (2002).
- [12] J.J. Lukkien, J.P.L. Segers, P.A.J. Hilbers, R.J. Gelten, and A.P.J. Jansen, *Phys. Rev. E* **58**, 2598 (1998).
- [13] O. Kortlüke, V.N. Kuzovkov, and W. von Niessen, *J. Chem. Phys.* **110**, 11523 (1999).
- [14] V.N. Kuzovkov, O. Kortlüke, and W. von Niessen, *Phys. Rev. Lett.* **83**, 1636 (1999).
- [15] A. von Oertzen, H. Rotermund, A. Mikhailov, and G. Ertl, *J. Phys. Chem. B* **104**, 3155 (2000).